Available online at www.sciencedirect.com
SCIENCE DIRECT®
Materials Research Bulletin 39 (2004) 297–308
Materials Research Bulletin
www.elsevier.com/locate/matresbu

Formation and electrophysical properties of Y-containing positive temperature coefficient of resistance ceramics doped by calcium, strontium, and manganese

Anatolii Belous*, Oleg V'yunov, Leonid Kovalenko

Solid State Department, V.I. Vernadskii Institute of General and Inorganic Chemistry, 32/34 prospekt Palladina, Kyiv 142 03680 Ukraine

Received 30 December 2002; received in revised form 8 April 2003; accepted 11 September 2003

Abstract

Formation, microstructure, and electrophysical properties of positive temperature coefficient of resistance ceramics of the systems $(Ba_{0.996}Y_{0.004})TiO_3$ and $(Ba_{0.746}Ca_{0.1}Sr_{0.15}Y_{0.004})TiO_3$ with manganese as acceptor dopant have been investigated. Is has been shown that manganese ions increase the potential barrier at grain boundaries and form a high-resistance outer layer in PTCR ceramics. The resistance of grains, outer layers and grain boundaries, and the value of the temperature coefficient of resistance as a function of the manganese content of positive temperature coefficient of resistance materials have been investigated.

Keywords: A. Ceramics; A. Semiconductors; C. Impedance spectroscopy; C. X-ray diffraction; D. Microstructure

1. Introduction

Positive temperature coefficient of resistance (PTCR) occurs in ceramics based on doped barium titanate near the temperature of phase transition from tetragonal ferroelectric to cubic paraelectric phase [1]. One of the conditions for arising PTCR effect is the formation of potential barriers at grain boundaries. Therefore, PTCR ceramics are synthesized in the conditions, where semiconducting grains and high-resistance grain boundaries are formed. In particular, this is achieved when rare-earth ions are partially substituted for barium ions and grain boundaries are oxidized during sintering the ceramic in air. The low order of resistivity change (ρ_{max}/ρ_{min}) in the PTCR region is one of the basic shortcomings of the use of barium-titanate-based PTCR materials in devices. It is known that the introduction of acceptor dopants in synthesized materials (for example, manganese) improves the above characteristic

* Corresponding author. Tel.: +380-44-444-3461; fax: +380-44-444-3070.
E-mail address: belous@ionc.kar.net (A. Belous).

0025-5408/$ – see front matter
doi:10.1016/j.materresbull.2003.09.031

of PTCR barium titanate [2,3]. The effect of manganese additive on the properties of PTCR materials based on barium titanate was investigated in a number of works [2–8]. It has been shown that manganese is placed at grain boundaries and acts as acceptor dopant increasing the order of resistivity change in the area of PTCR effect [2]. Introduction of manganese in the PTCR ceramics based on barium titanate changes the energy of acceptor states [4,5]. Manganese forms a number of associates with oxygen vacancies, which act as the acceptor-like centers of electron capture [6]. In the case of partial substitution of titanium ions by manganese ions in barium titanate the samples become bimodal at manganese contents of over 1 mol%, and in the range of 0.5–1.7 mol% the coexistence of tetragonal and hexagonal phases of the perovskite is observed [7]. In the case of partial substitution of barium ions by strontium ions in barium titanate the range of coexistence of tetragonal and hexagonal phases is shifted towards higher Mn concentration [8]. Manganese dopant affects PTCR effect to a large extent due to the fact that the redox transformations of manganese and redox processes in PTCR ceramics, accompanied by the partial $Ti^{4+} \leftrightarrow Ti^{3+}$ transformation, occur in one temperature interval [9]. However, the information about the distribution of manganese dopant in polycrystalline material is scantily presented in the literature.

Therefore, the aim of this work was to study the distribution of manganese ions and its effect on the properties of grains, outer grain layers and grain boundaries of yttrium-doped barium titanate $(Ba_{0.996}Y_{0.004})TiO_3$ and solid solution with partial isovalent substitution in barium sites $(Ba_{0.746}Ca_{0.1}Sr_{0.15}Y_{0.004})TiO_3$.

2. Experimental

PTCR materials with yttrium as donor dopant ($(Ba_{0.996}Y_{0.004})TiO_3$) and with partial isovalent substitution in barium sites ($(Ba_{0.746}Ca_{0.1}Sr_{0.15}Y_{0.004})TiO_3$) were used for the investigation. Whereas yttrium can reside in both titanium and barium sites [10], in the present work to provide the incorporation of yttrium in barium sublattice a small excess of titanium was used. The concentration of yttrium was much lower then its solubility limit in barium sublattice (~1.5 at.%) [11]. Neither bimodal microstructure nor coexistence of tetragonal and hexagonal phases are not observed in the samples because of the low manganese concentration used [7]. Extra-pure $BaCO_3$, $CaCO_3$, $SrCO_3$, TiO_2, Y_2O_3, SiO_2, $MnSO_4$, and water solution of ammonia were used as starting reagents. Powders were ball-milled in agate mortar. In order to reduce the pollution of mixed powders during milling, the working surfaces of crushing cylinders were covered with vacuum rubber. Uniform distribution of manganese dopant was achieved by its precipitation from solutions. Powder X-ray diffraction (PXRD) patterns were collected on a DRON-4-07 diffractometer using Cu Kα radiation in the angular range $2\theta = 10-150^\circ$ in a step-scan mode with a step size of 0.02° and a counting time of 10 s per data point. As external standards, we used SiO_2 (2θ calibration) and Al_2O_3 (NIST SRM1976 intensity standard [12]). Structural parameters and phase composition were determined by the Rietveld profile analysis method, using the FullProf program and Powder Diffraction File data. Electrophysical properties of samples sintered at 1340–1360 °C in air have been investigated. The densities of ceramic samples were calculated by the Archimedes method and were found to be 92–94% of the theoretical value. The grain sizes in the ceramics were determined using X-ray microanalyzer JCXA Superprobe 733 (JEOL, Japan). Aluminum electrodes were fabricated by burning in Al paste. Electrical properties of the ceramics were studied with the direct and alternating current. Impedance analyzer PGSTAT-30 (Solartron) was

used for the measurements in the frequency range 1 Hz–1 MHz, and BM-560 Q-meter was used for measurements in the frequency range 50 kHz–35 MHz. Equivalent circuit and values of its components were determined using the Frequency Response Analyser 4.7 PC program.

3. Results and discussion

In order to define the intermediate phases, which are formed when synthesizing $BaTiO_3$-based PTCR ceramics by solid state reactions technique, the heat treatment of the powders in an isothermal mode over the temperature range of 600–1100 °C was carried out. XRPD patterns of the powders $(Ba_{0.996}Y_{0.004})TiO_3$ fired at the temperatures lower than the calcination temperature (1100 °C) contain reflexes of several phases. The perovskite phase was the dominant one within the entire temperature range. The intermediate phases of the synthesis of yttrium-doped barium titanate $(Ba_{0.996}Y_{0.004})TiO_3$ were barium orthotitanate (Ba_2TiO_4) and barium tetratitanate ($BaTi_4O_9$). Beside Ba_2TiO_4 and $BaTi_4O_9$, the additional intermediate phases accompanying the synthesis of yttrium-doped barium titanate $(Ba_{0.746}Ca_{0.1}Sr_{0.15}Y_{0.004})TiO_3$ were the phases $Ca_3Ti_2O_7$ and $Sr_4Ti_3O_{10}$. After the heat treatment over 1100 °C all the samples examined were single-phase ones within the accuracy of the PXRD method, which is ca. 2 mol%.

Ceramic samples $(Ba_{0.996}Y_{0.004})TiO_3$ and $(Ba_{0.746}Ca_{0.1}Sr_{0.15}Y_{0.004})TiO_3$ after sintering at 1360 °C in air have the perovskite structure with space group *P4mm* (Ba(Y) 1b (1/2 1/2 *z*); Ti 1a (0 0 0); O_1 1a (0 0 *z*); O_2 2c (1/2 0 *z*) [13]). XRPD has detected no Mn-containing compounds in the samples doped with $MnSO_4$. The parameters of the crystal structure of the ceramic samples were determined by means of Rietveld full-profile X-ray analysis (Fig. 1). The introduction of manganese dopant slightly affects unit cell parameters of the samples studied (Table 1).

Electron micrographs of $(Ba_{0.996}Y_{0.004})TiO_3$ ceramic sintered in air for 2 h are shown in Fig. 2a and b. The average grain size of barium-titanate-based ceramic is ca. 35 μm. Partial substitution of strontium for barium essentially diminishes the grain size. Partial substitution of calcium for barium has a weaker effect on the decrease in grain size in comparison with strontium substitution. Combined

Table 1
Some structural parameters of the PTCR ceramics investigated

Composition	$(Ba_{0.996}Y_{0.004})TiO_3$		$(Ba_{0.746}Ca_{0.1}Sr_{0.15}Y_{0.004})TiO_3$	
	Without manganese	+0.006 mol% Mn	Without manganese	+0.006 mol% Mn
Unit cell parameters				
a (Å)	3.9929(1)	3.9932(3)	3.9625(2)	3.9636(2)
c (Å)	4.0356(1)	4.0346(3)	3.9917(3)	3.9911(2)
V (Å^3)	64.339(3)	64.335(8)	62.675(6)	62.701(6)
Positions of ions (*z*/*c*)				
Ba-site ions	0.511(7)	0.522(8)	0.530(7)	0.519(9)
O_1	0.44(1)	0.49(2)	0.45(1)	0.45(1)
O_2	0.04(1)	0.06(2)	0.07(1)	0.03(4)
Agreement factors				
R_b (%)	3.89	4.27	3.17	4.24
R_f (%)	2.98	2.97	2.75	4.36

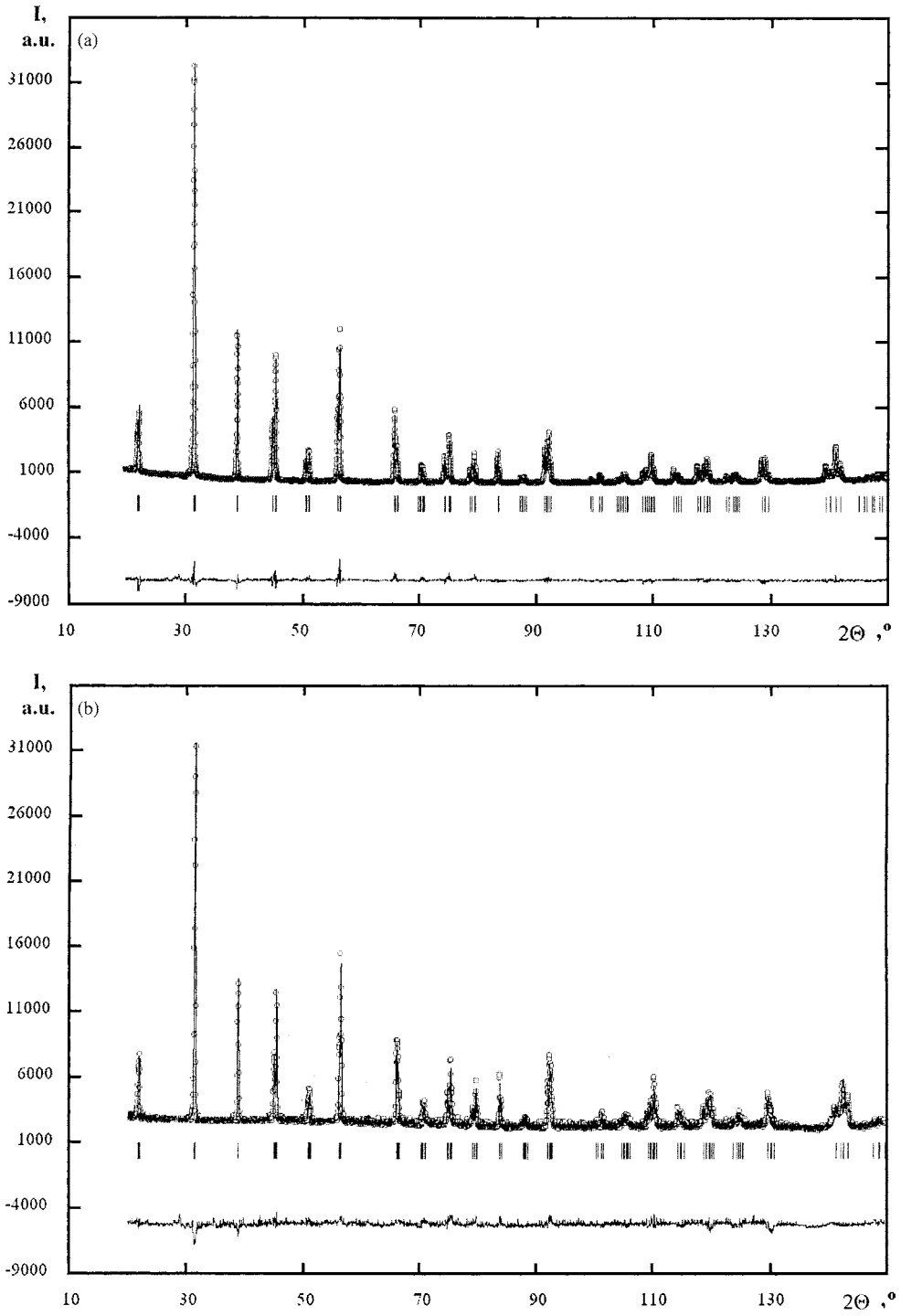

Fig. 1. Experimental (dot) and calculated (line) room-temperature powder X-ray diffraction patterns of $(Ba_{0.996}Y_{0.004})TiO_3$ (a) and $(Ba_{0.746}Ca_{0.1}Sr_{0.15}Y_{0.004})TiO_3$ (b) ceramics. Bars indicate the peak positions. Difference curves are shown below.

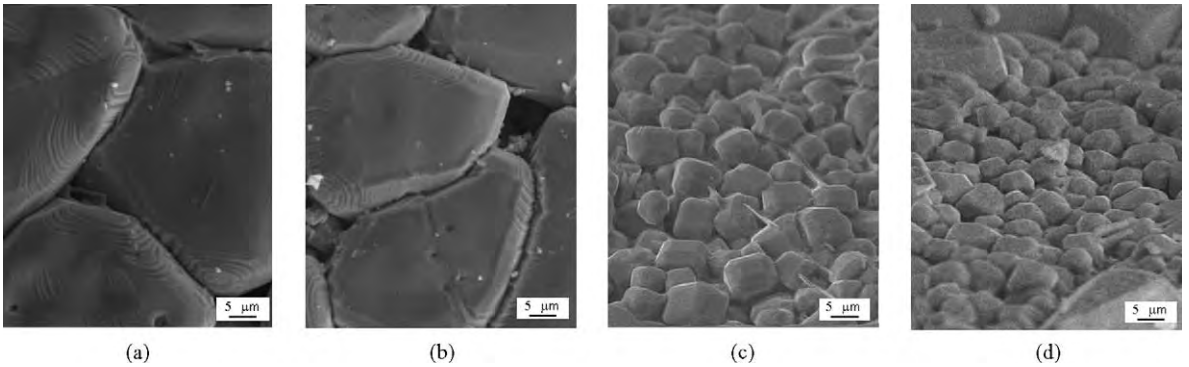

Fig. 2. Microstructure of the PTCR ceramics $(Ba_{0.996}Y_{0.004})TiO_3$ (a); $(Ba_{0.996}Y_{0.004})TiO_3 + 0.006$ mol% Mn (b); $(Ba_{0.746}Ca_{0.1}Sr_{0.15}Y_{0.004})TiO_3$ (c); and $(Ba_{0.746}Ca_{0.1}Sr_{0.15}Y_{0.004})TiO_3 + 0.006$ mol% Mn (d). Scale bar = 10 μm.

introduction of calcium and strontium into the barium sublattice of barium titanate makes an additional effect on the microstructure, forming close-grained (ca. 5 μm) ceramics with uniform distribution of grain sizes (Fig. 2c and d).

The temperature dependence of resistivity of the PTCR ceramics can be divided schematically into three ranges (Fig. 3). Range I extends from room temperature up to the phase transition temperature, and is characterizes by relatively low resistivity, which decreases with the temperature (the temperature dependence demonstrates semiconductor behavior). Range II is situated over the phase transition temperature, where the rapid growth of resistivity is observed (PTCR effect). Range III exists at higher temperatures, and is characterized by high resistivity, which decreases with the temperature. When PTCR ceramics based on barium titanate are doped with manganese, the order of resistivity change in the PTCR area increases (See Fig. 3, range II).

To ascertain the reasons of the increase in the order of resistance change in the PTCR region of ceramics as a function of manganese content, the temperature dependence of the potential barrier at the grain boundary and the characteristics of materials in the temperature ranges near the PTCR range have been calculated using equations derived in Refs. [1,14,15]. In region I (Fig. 3), the temperature dependence of resistivity is described by the equation [14,15]:

$$\rho_s = \rho_0^{\mathrm{I}} \exp\left(\frac{E_a^{\mathrm{I}}}{kT}\right) \tag{1}$$

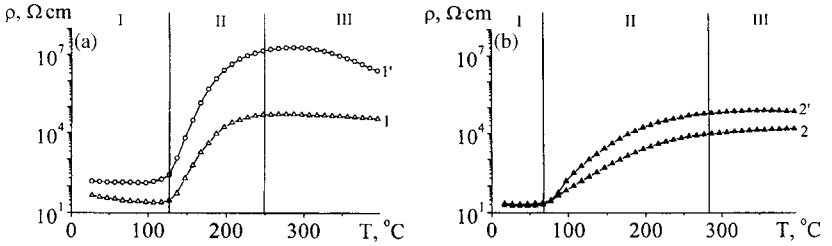

Fig. 3. Resistivity (ρ) of the PTCR ceramics $(Ba_{0.996}Y_{0.004})TiO_3$ (1); $(Ba_{0.996}Y_{0.004})TiO_3 + 0.006$ mol% Mn (1′); $(Ba_{0.746}Ca_{0.1}Sr_{0.15}Y_{0.004})TiO_3$ (2); and $(Ba_{0.746}Ca_{0.1}Sr_{0.15}Y_{0.004})TiO_3 + 0.006$ mol% Mn (2′) vs. temperature. I, II, and III are the ranges with different character of dependences $\rho(T)$.

where ρ_0^{I} is a constant for barium titanate [15], E_a^{I} is the activation energy for conduction in region I, and k is the Boltzmann constant (1.38×10^{-23} J/K $= 8.62 \times 10^{-5}$ eV/K).

A similar equation is applicable to the region III [1,14]:

$$\rho_d = \rho_0^{\mathrm{III}} \exp\left(\frac{E_a^{\mathrm{III}}}{kT}\right) \tag{2}$$

where E_a^{III} is the activation energy for conduction in region III.

The temperature dependence of resistivity in region II, where PTCR effect occurs, is commonly interpreted using Heywang model [14]:

$$\rho = \frac{\alpha \rho_s \exp(\Phi_0(T))}{kT} \tag{3}$$

where α is a geometric factor and $\Phi_0(T)$ is the intergranular barrier height:

$$\Phi_0(T) = \frac{e^2 n_{\mathrm{D}} b^2}{2\varepsilon_i(T)\varepsilon_0} \tag{4}$$

Here e is the charge of electron (1.602×10^{-19} C), n_{D} is the bulk electron concentration, b is the potential barrier thickness ($2b = n_{\mathrm{S}}/n_{\mathrm{D}}$, where n_{S} is the surface concentration of acceptor states), and $\varepsilon_i(T)$ is the permittivity of the grain bulk. In ferroelectrics, $\varepsilon_i(T)$ follows the Curie–Weiss law: $\varepsilon_i(T) = C/(T-\Theta)$, where C is the Curie constant and Θ is the Curie temperature (in barium titanate $C = 1.7 \times 10^5$ K; $\Theta = 383$ K [14]).

Assuming that the temperature dependence of the permittivity of grain boundaries follows the Curie–Weiss law [1], Eqs. (1) and (3) result in:

$$\rho = \alpha \rho_0 \exp\left(\frac{E_a^{\mathrm{I}}}{kT}\right) \exp\left(\frac{e^2 n_{\mathrm{D}} b^2 (T-\Theta)}{2\varepsilon_0 C k T}\right) \tag{5}$$

Pre-exponentials in the ranges I (ρ_0^{I}) and III (ρ_0^{III}), which are the constants of a material, and activation energies E_a^{I} and E_a^{III} are listed in Table 2. Products of donor concentration n_{D} and potential barrier thickness b, which determine the characteristics of potential barriers at grain boundaries in the paraelectric temperature range, were also calculated from the experimental data, and are listed in Table 2. Results of the calculations for the $(Ba_{0.996}Y_{0.004})TiO_3$ and $(Ba_{0.746}Ca_{0.1}Sr_{0.15}Y_{0.004})TiO_3$ ceramics show that in the temperature range I the ρ_0^{I} value increases and the activation energy E_a^{I} decreases with increasing manganese content, whereas in the temperature range III the ρ_0^{III} value decreases and the activation energy E_a^{III} increases. Deriving from the data obtained, the potential barrier at the grain boundary (Φ_0) of PTCR ceramics as a function of manganese content in the temperature range II has been calculated (Fig. 4b). As it is evident from the data presented, the magnitude of the potential barrier increases with the manganese content of PTCR ceramics, which accounts for the increase in the order of resistance change in the PTCR region (Fig. 3).

The results of frequency investigation of the PTCR ceramics $(Ba_{0.996}Y_{0.004})TiO_3 + y$ mol% Mn and $(Ba_{0.746}Ca_{0.1}Sr_{0.15}Y_{0.004})TiO_3 + y$ mol% Mn can be analyzed from four types of dependences: complex impedance (Z^*), complex admittance (Y^*), complex permittivity (ε^*), and complex electric modulus (M^*) [16–18]. The complex quantities are interrelated: $M^* = 1/\varepsilon^* = j\omega \mathrm{Co} Z^* = j\omega \mathrm{Co}(1/Y^*)$ (where $j = (-1)^{1/2}$). Initially, the results of frequency investigation of PTCR materials were obtained as $Z'' = f(Z')$ relations (Fig. 5a). This plot is convenient for the determination of components of the

Table 2
Effect of manganese content on the characteristics of temperature dependences of the resistance of the PTCR ceramics $(Ba_{0.996}Y_{0.004})TiO_3$ and $(Ba_{0.746}Ca_{0.1}Sr_{0.15}Y_{0.004})TiO_3$ in various temperature ranges

Manganese content, y (mol%)	Range I		Range II	Range III	
	ρ_0^{I} (Ω cm)	E_a^{I} (eV)	$n_D b^2$ (cm^{-1})	ρ_0^{III} (Ω cm)	E_a^{III} (eV)
$(Ba_{0.996}Y_{0.004})TiO_3 + y$ mol% Mn					
0	4.6	0.09	9.1×10^8	3254	0.20
0.002	17.9	0.06	9.3×10^8	106	0.59
0.004	21.3	0.06	9.3×10^8	76.0	0.70
0.006	27.4	0.06	9.8×10^8	15.2	0.75
0.008	45.9	0.05	1.2×10^9	1.2	0.91
0.010	61.4	0.05	1.2×10^9	2.7	0.85
0.012	104	0.04	1.3×10^9	3.0	0.85
$(Ba_{0.746}Ca_{0.1}Sr_{0.15}Y_{0.004})TiO_3 + y$ mol% Mn					
0	12.8	0.04	3.2×10^8	6082	0.13
0.002	14.3	0.04	3.6×10^8	2433	0.22
0.006	14.6	0.04	4.2×10^8	365	0.36
0.01	15.8	0.04	5.4×10^8	110	0.44
0.02	17.6	0.04	5.5×10^8	2.1	0.69
0.03	24.9	0.04	5.8×10^8	1.5	0.72

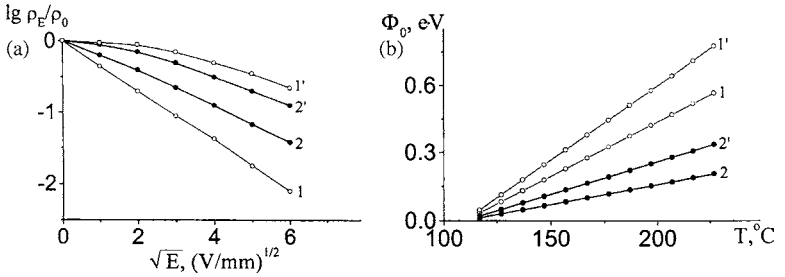

Fig. 4. $(Ba_{0.746}Ca_{0.1}Sr_{0.15}Y_{0.004})TiO_3$–$(Ba_{0.746}Ca_{0.1}Sr_{0.15}Y_{0.004})TiO_3$ potential barrier (Φ_0) at grain boundaries of the PTCR ceramics $(Ba_{0.996}Y_{0.004})TiO_3$ (1); $(Ba_{0.996}Y_{0.004})TiO_3 + 0.006$ mol% Mn (1′); $(Ba_{0.746}Ca_{0.1}Sr_{0.15}Y_{0.004})TiO_3$ (2); $(Ba_{0.746}Ca_{0.1}Sr_{0.15}Y_{0.004})TiO_3 + 0.006$ mol% Mn (2′) vs. temperature.

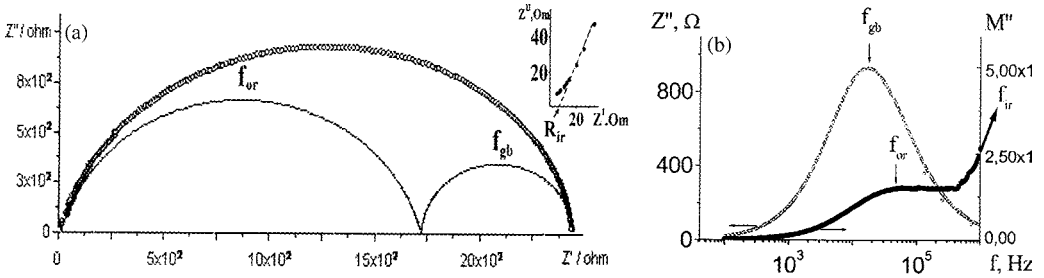

Fig. 5. Complex impedance plot ($Z'' = f(Z')$) (a) and combined impedance (Z'') and modulus (M'') spectroscopic plots (b) for PTCR $(Ba_{0.996}Y_{0.004})TiO_3$; inner grain region marked as "ir," outer grain region marked as "or," grain boundary marked as "gb."

equivalent circuit. For the further analysis, the results of investigation of complex impedance were also represented as frequency dependencies of the imaginary components of complex impedance Z'' and complex electric modulus M'' (Fig. 5b). In the case of parallel RC element, the frequency dependencies of Z'' and M'' are described by the equations [16–18]:

$$Z'' = R\frac{\omega RC}{1+(\omega RC)^2} \tag{6}$$

$$M'' = \frac{\varepsilon_0}{C}\frac{\omega RC}{1+(\omega RC)^2} \tag{7}$$

where $\omega = 2\pi f$ (f = frequency in Hz), and ε_0 is the permittivity (8.854×10^{-14} F cm^{-1}).

From Eqs. (6) and (7), it follows that:

$$\omega_{max} = \frac{1}{RC} \tag{8}$$

$$Z''_{max} = \frac{R}{2} \tag{9}$$

$$M''_{max} = \frac{\varepsilon_0}{2C} \tag{10}$$

Eqs. (8)–(10) show that the shift in the positions of Z''_{max} and M''_{max} at the frequency axis are associated with a change in the values of both capacity and resistance in the corresponding RC element.

Fig. 4 shows that the peaks Z''_{max} and M''_{max} do not coincide in frequency. This indicates that the positions of the above maximums are determined by the various areas of the ceramics [16–18]. We interpreted experimental results by using the model of PTCR ceramics' grain proposed by Sinclair and West [19]. According to this model, the inner fraction of a grain has semiconducting properties whereas the grain boundaries have dielectric properties. Between these two areas the transition region occurs which has the resistivity higher than that of semiconducting inner region, but lower than that of the grain boundary dielectric layer. There can be various origins of the formation of this transition layer, for example, oxygen diffusion into the grains when sintering the ceramics, introduction of acceptor dopants (including manganese one), etc. These areas of the ceramics are electrically non-uniform and can be represented by an equivalent circuit, which includes three parallel RC-elements connected in series. In particular, the change in the value and positions of maximums of $Z''(f)$ and $M''(f)$ are determined by the electrophysical properties of the following fractions of a grain: grain boundaries determine the plot $Z''(f)$, grain outer layer is responsible for the plot $Z''(f)$ in the middle of the measuring frequency range, whereas inner grain determines the plot of $M''(f)$ at the frequencies over 10^8 Hz. These areas can also be distinguished using the plot $Z'' = f(Z')$ (see Fig. 5a).

Resistances and capacitances of grain, outer layer and grain boundary of the PTCR ceramics $(Ba_{0.996}Y_{0.004})TiO_3$ and $(Ba_{0.746}Ca_{0.1}Sr_{0.15}Y_{0.004})TiO_3$ without manganese dopant were calculated from the experimental data (Figs. 6 and 7 respectively). The temperature dependence of outer layer resistance of $(Ba_{0.996}Y_{0.004})TiO_3$ ceramic is of the character similar to that of grain and demonstrates no anomalies (Fig. 6a, curves 2 and 3), whereas that of grain boundary displays the anomalies. Formation of outer layer in the PTCR ceramics without manganese dopant occurs due to the diffusion of oxygen into the grains on cooling. In this case, the trivalent titanium ions partially change to tetravalent ones in outer layer, resulting in an increase in the electrical resistivity of this layer [20]. Hence, the PTCR effect

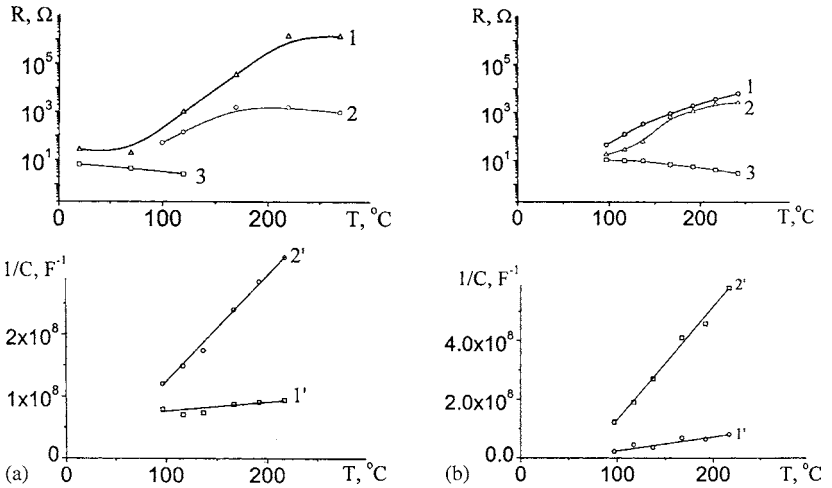

Fig. 6. Resistance of grain boundary (1), outer layer (2), and grain (3), inverse capacitance of grain boundary (1′) and outer layer (2′) of the PTCR ceramics $(Ba_{0.996}Y_{0.004})TiO_3$ (a) and $(Ba_{0.746}Ca_{0.1}Sr_{0.15}Y_{0.004})TiO_3$ (b) vs. temperature.

in $(Ba_{0.996}Y_{0.004})TiO_3$ ceramic without manganese dopant occurs due to a change in electrophysical properties of grain boundaries (Fig. 6a, curve 1). Unlike $(Ba_{0.996}Y_{0.004})TiO_3$, the temperature dependence of outer layer resistance of the $(Ba_{0.746}Ca_{0.1}Sr_{0.15}Y_{0.004})TiO_3$ ceramic is of the character similar to that of grain boundary (Fig. 6b, curves 1 and 2). The PTCR effect in $(Ba_{0.746}Ca_{0.1}Sr_{0.15}Y_{0.004})TiO_3$ ceramics without manganese dopant occurs due to the change in electrophysical properties of both outer layers and grain boundaries. The capacitance of grain boundaries of the PTCR ceramics $(Ba_{0.996}Y_{0.004})TiO_3$ and $(Ba_{0.746}Ca_{0.1}Sr_{0.15}Y_{0.004})TiO_3$ reaches high values and slightly

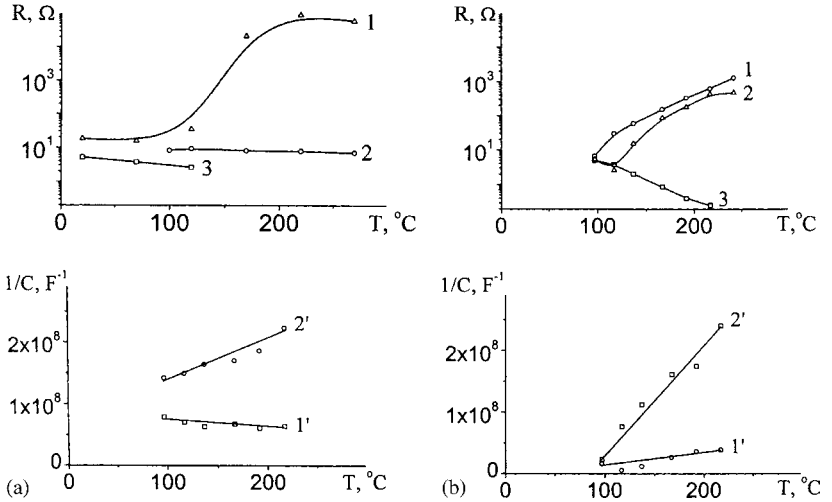

Fig. 7. Resistance of grain boundary (1), outer layer (2), and grain (3), inverse capacitance of grain boundary (1′) and outer layer (2′) of the PTCR ceramics $(Ba_{0.996}Y_{0.004})TiO_3 + 0.006$ mol% Mn (a) and $(Ba_{0.746}Ca_{0.1}Sr_{0.15}Y_{0.004})TiO_3 + 0.006$ mol% Mn (b) vs. temperature.

changes with temperature. Above the phase transition temperature, the capacitance of outer layer varies with temperature in accordance with Curie–Weiss law.

The resistance of grain, outer layer and grain boundary of the PTCR ceramics $(Ba_{0.996}Y_{0.004})TiO_3$+ 0.006 mol% Mn and $(Ba_{0.746}Ca_{0.1}Sr_{0.15}Y_{0.004})TiO_3 + 0.006$ mol% Mn is shown in Fig. 7. The character of the variation of outer layer resistance of the ceramic $(Ba_{0.996}Y_{0.004})TiO_3 + 0.006$ mol% Mn with the temperature is similar to that of the variation of grain boundary resistance, contrary to the ceramics without manganese dopant (Fig. 7a, curves 2 and 3). Introducing manganese dopants in $(Ba_{0.746}Ca_{0.1}Sr_{0.15}Y_{0.004})TiO_3$ ceramic increases slightly the resistance of both the outer layer and grain boundary (Fig. 7b). The capacitance of grain boundary depends slightly on temperature in the PTCR ceramics $(Ba_{0.996}Y_{0.004})TiO_3 + 0.006$ mol% Mn and $(Ba_{0.746}Ca_{0.1}Sr_{0.15}Y_{0.004})TiO_3 + 0.006$ mol% Mn, whereas the slope of the curve $2'$ decreases (Fig. 7). This is, probably, due to the fact that manganese partially diffuses into the grain outer layer [21].

The results of the investigation of the properties of the PTCR $(Ba_{0.996}Y_{0.004})TiO_3$ and $(Ba_{0.746}Ca_{0.1}Sr_{0.15}Y_{0.004})TiO_3$ ceramics at room temperature as a function of manganese content are shown in Fig. 8. As it is evident from the data presented, when the manganese content of PTCR ceramics is increased, the grain boundary resistance increases, whereas the total grain and outer layer resistance remains practically unchanged. The resistance and capacitance of grain and the grain outer layer of PTCR barium titanate cannot be distinguished at room temperature due to the small difference in their values. At the same time, the difference in resistance between grain and the grain outer layer of PTCR ceramics becomes more pronounced with rising temperature. The capacitance of grain boundaries of the PTCR ceramics $(Ba, Y)TiO_3 + y$ mol% Mn (a) and $(Ba_{0.746}Ca_{0.1}Sr_{0.15}Y_{0.004})TiO_3 + y$ mol% Mn decreases with increasing manganese content, and the total capacitance of grain and the outer layer increases (see Fig. 8). The total capacitance of grain and the grain outer layer of the PTCR ceramic $(Ba_{0.996}Y_{0.004})TiO_3 + y$ mol% Mn depends on manganese content more stronger than that of $(Ba_{0.746}Ca_{0.1}Sr_{0.15}Y_{0.004})TiO_3 + y$ mol% Mn (curve $2'$).

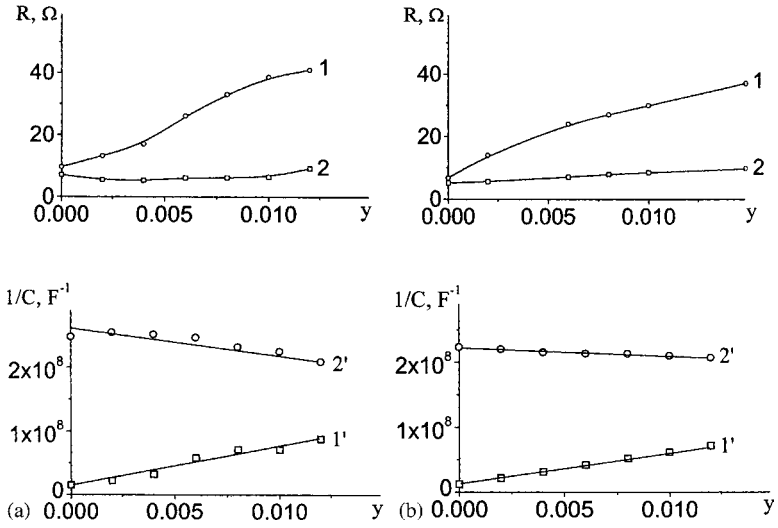

Fig. 8. Resistance of grain boundary (1), total resistance of outer layer and grain (2), inverse capacitance of grain boundary ($1'$) and total capacitance of outer layer and grain ($2'$) of the PTCR ceramics $(Ba_{0.996}Y_{0.004})TiO_3 + y$ mol% Mn (a) and $(Ba_{0.746}Ca_{0.1}Sr_{0.15}Y_{0.004})TiO_3 + y$ mol% Mn (b) vs. manganese content; $T_{meas} = 20\,^{\circ}C$.

4. Conclusion

Thus, the investigations of the manganese-doped PTCR ceramics $(Ba_{0.996}Y_{0.004})TiO_3$ and $(Ba_{0.746}Ca_{0.1}Sr_{0.15}Y_{0.004})TiO_3$ carried out by us over a wide frequency and temperature range showed that:

1. PTCR ceramic of $(Ba_{0.996}Y_{0.004})TiO_3$ system has a coarse-grained microstructure. When adding manganese dopant the manganese ions diffuse into a grain essentially changing the properties of grain outer layers. At the same time, the electrophysical properties of inner grain and grain boundaries change slightly.
2. In the case of PTCR materials of the $(Ba_{0.746}Ca_{0.1}Sr_{0.15}Y_{0.004})TiO_3$ system, fine-grained ceramics are formed. Hence, the specific surface of the grains in the $(Ba_{0.746}Ca_{0.1}Sr_{0.15}Y_{0.004})TiO_3$ system is much larger than that in the $(Ba_{0.996}Y_{0.004})TiO_3$ system. Therefore, at equal concentrations of manganese, the surface density of manganese ions is lower in the materials of the $(Ba_{0.746}Ca_{0.1}Sr_{0.15}Y_{0.004})TiO_3$ system. In this case, the manganese ions affect slightly the properties of transition layer and, hence, the electrophysical properties of the $(Ba_{0.746}Ca_{0.1}Sr_{0.15}Y_{0.004})TiO_3$ ceramics.
3. It has been shown that the impedance spectroscopy allows the ascertainment of the dopant distribution of (in particular, manganese) in the grains, that is important for the development of materials with high-level technical characteristics.

References

[1] W. Heywang, Resistivity anomaly in doped barium titanate, J. Am. Ceram. Soc. 47 (10) (1964) 484–490.
[2] H.M. Al-Allak, A.W. Brinkman, G.J. Russel, J. Woods, The effect of Mn on the positive temperature coefficient of resistance characteristics of donor doped $BaTiO_3$ ceramics, J. Appl. Phys. 63 (9) (1988) 4530–4535.
[3] J.H. Lee, S.H. Kim, S.H. Cho, Valence change of Mn ions in $BaTiO_3$-based PTCR materials, J. Am. Ceram. Soc. 78 (10) (1995) 2845–2848.
[4] B. Huybrechts, K. Ishizaki, M. Takata, Experimental evaluation of the acceptor states compensation in PTC-type barium titanate, J. Am. Ceram. Soc. 75 (1992) 722.
[5] B. Huybrechts, M. Takata, K. Ishizaki, Grain boundary oxidation of semiconductive Mn-doped $BaTiO_3$, Ceram. Transact. Am. Ceram. Soc. 44 (1994) 151–160.
[6] T. Miki, A. Fudjimoto, S. Jida, An evidence of trap activation for positive temperature coefficient of resistivity in $BaTiO_3$ ceramics with substitutional Nb and Mn as impurities, J. Appl. Phys. 83 (3) (1998) 1592–1603.
[7] H.T. Langhammer, T. Muller, K.-H. Felgner, H.-P. Abich, Crystal structure and related properties of manganese-doped titanate ceramics, J. Am. Ceram. Soc. 83 (3) (2000) 605–611.
[8] H.T. Langhammer, T. Muller, K.-H. Felgner, H.-P. Abich, Influence of strontium on manganese-doped barium titanate ceramics, Mater. Lett. 42 (2000) 21–24.
[9] Yu.D. Kostikov, B.B. Leikina, Effect of Transition 3d-metal oxides on PTCR properties of ceramics based on semiconducting barium titanate, Inorg. Mater. 26 (4) (1990) 884–886.
[10] L.A. Xue, Y. Chen, R.J. Brook, The influence of ionic radii on the incorporation of trivalent dopants into $BaTiO_3$, Mater. Sci. Eng. B1 (1988) 193–201.
[11] J. Zhi, A. Chen, Y. Zhi, P.M. Vilarihno, J.L. Baptista, Incorporation of yttrium in barium titanate ceramics, J. Am. Ceram. Soc. 82 (5) (1999) 1345–1348.
[12] Certificate of Analysis, Standard Reference Material 1976, Instrument Sensitivity Standard for X-ray Powder Diffraction, National Institute of Standards & Technology, Gaithersburg, 1991, p. 1–4.
[13] H.T. Evans, An X-ray diffraction study of tetragonal barium titanate, Acta Cryst. 14 (1961) 1019–1026.
[14] W. Heywang, Semiconducting barium titanate, J. Mater. Sci. 6 (1971) 1214–1226.

[15] D.Y. Wang, K. Umeya, Electrical properties of PTCR barium titanate, J. Am. Ceram. Soc. 73 (3) (1990) 669–677.
[16] D.C. Sinclair, F.D. Morrison, A.R. West, Applications of combined impedance and electric modulus spectroscopy to characterise electroceramics, Int. Ceram. 2 (2000) 33–37.
[17] F.D. Morrison, D.C. Sinclair, A.R. West, An alternative explanation for the origin of the resistivity anomaly in La-doped $BaTiO_3$, J. Am. Ceram. Soc. 84 (2) (2001) 474–476.
[18] F.D. Morrison, D.C. Sinclair, A.R. West, Characterization of lanthanum-doped barium titanate ceramics using impedance spectroscopy, J. Am. Ceram. Soc. 84 (3) (2001) 531–538.
[19] D.C. Sinclair, A.R. West, Use of succinic acid to test the stability of PTCR barium titanate ceramics under reducing conditions, J. Am. Ceram. Soc. 78 (1) (1995) 241–244.
[20] F.D. Morrison, A.M. Coats, D.C. Sinclair, A.R. West, Charge compensation mechanism in La-doped $BaTiO_3$, J. Electroceram. 6 (3) (2001) 219–232.
[21] K. Altbersen, D. Hennings, O. Steigelmann, Donor-acceptor charge complex formation in barium titanate ceramics: role of firing atmosphere, J. Electroceram. 2/3 (1998) 193–198.